Journal of Thermal Analysis and Calorimetry (2023) 148:12739–12750
https://doi.org/10.1007/s10973-023-12572-9

Preparation and combustion performance of molecular perovskite energetic material DAP-4-based composite with Titanium powder

Kaili Liang[1,2] · Yang Liu[1] · Lishuang Hu[1] · Jiashun Liang[1] · Tiancheng Lv[1] · Wei Wu[1] · Yanping Wang[3] · Zhiqiong Tu[4] · Shuangqi Hu[1]

Received: 29 October 2022 / Accepted: 18 September 2023 / Published online: 10 October 2023

Abstract
Micron-sized titanium particles have potential applications as energetic metal high-enthalpy fuel materials. The molecular perovskite energetic material DAP-4 $(H_2dabco)[NH_4(ClO_4)_3]$ is a potential high-energy oxidizer in solid rocket propellants. To explore the combustion mechanism and energy output of DAP-4-based Ti composites, the combustion characteristics of DAP-4/Ti and F/DAP-4/Ti were studied by electrode ignition device. The results show that the burning rate of DAP-4 can be adjusted by controlling the mass ratio of DAP-4/Ti. After adding Ti into DAP-4, the heat release, self-sustaining combustion time and flame front propagation velocity are greatly increased to 9,113 J g^{-1}, 265 ms and 0.225 mm ms^{-1}, respectively, better than those of DAP-4. With Ti added, the decomposition peak temperature of F/DAP-4/Ti dropped from 381.5 to 360.4 ℃. The experimental results contribute to a better understanding of the chemical reaction mechanism and energy release characteristics of DAP-4-based propellants containing Ti.

Keywords Ti particles · Molecular perovskite · Combustion characteristics · Decomposition

Introduction

In order to improve the energy density and combustion stability of solid propellants, adjust the combustion speed and energy output, and further develop its broader application potential [1–3], adding micron-metal particles (MPs) to adjust the combustion performance of fuels has become a research hotspot [4–8]. Particles such as Al, B, Mg, Zr, Zn, etc., have been potential fuels for composite propellants in recent years [9–11]. The novel properties exhibited by micron-sized materials, such as higher combustion enthalpy and larger specific surface area, enable significant optimization of both energy release and reactive centers [12].

Molecular perovskite energetic materials have a special crystal structure with a cubic that allows for tunable catalytic activity and high thermal stability [13]. Since 2018, Chen et al. [14] designed and prepared a high-energy compound molecule $(H_2dabco)[M(ClO_4)_3]$ ($M = Na^+$, K^+, Rb^+, and NH_4^+). $(H_2dabco)[NH_4(ClO_4)_3]$ is the only metal-free perovskite high-energy material that combines AP as the basic unit with low-cost organic fuels (triethylenediamine). However, the detonation speed and thermal stability, oxygen delivery capacity and energy release of DAP-4 are far superior to AP. In recent years, Deng et al. [15] discovered that molecular perovskite energetic materials can be used as potential energetic oxidizers for solid rocket propellants, and that adding Al to DAP-4 can enhance the combustion performance of propellants. The study by Zhou et al. [16] showed that the thermal stability of DAP-4 is better than most of the currently used energetic materials. Li et al. [17–20] showed that CoFe-500, MoS_2 nanosheets, functionalized graphene, and Ti_3C_2 MXene additives can enhance the thermal decomposition of ammonium perchlorate-based molecular perovskites.

✉ Lishuang Hu
hlsly1314@163.com

✉ Yanping Wang
gloria_716@163.com

1 School of Environment and Safety Engineering, North University of China, Taiyuan 030051, People's Republic of China

2 Shanxi Jiangyang Xing'an Industrial Explosive Materials Co., Ltd, Taiyuan 030041, People's Republic of China

3 Explosive Engineering and Safety Technology Research Institute of Ordnance Industry, Beijing 100053, People's Republic of China

4 Shanxi North Xing'an Chemical Industry Co., Ltd, Taiyuan 030008, People's Republic of China

Titanium is a fuel with a strong oxidizer. Ti has a higher normalized enthalpy of combustion per unit volume compared to Al [21–23]. The advantages of high energy density, high activity, high strength, corrosion resistance, and non-toxicity make Ti-MPs a viable alternative fuel source [24]. Titanium particles have a low ignition point and burn relatively slowly, with combustion times an order of magnitude longer than those of Mg particles of the same size. The long combustion times indicate that the titanium particles actually burn on the surface rather than in the gas as a vapor [25, 26]. It can be reasonably expected that the eruption of the mixture of titanium and oxidant can generate TiO_2 cloud, and only part of the oxidized particles are sprayed out and react with the surrounding gas. Exploring the combustion flame and exothermic decomposition of DAP-4 becomes extremely attractive when considering the possible effects of Ti-MPs and their oxides on ignition mechanics.

In this paper, the ignition and combustion mechanism of molecular perovskite energetic material DAP-4-based Ti composites under electrode ignition were investigated. Samples of DAP-4/Ti and F/DAP-4/Ti were successfully designed and prepared. The morphological and structural characterization of the raw materials and samples were carried out, and the heat release and pressure variation of pure DAP-4 and hybrid powder were tested. The flame propagation of the hybrid powders and composites was observed using self-assembled molds and high-speed photographic cameras. And the effect of titanium powder addition on the thermal decomposition of DAP-4 was analyzed by TG-DSC. The collected combustion products were also characterized and tested to add reliability to the proposed mechanism. A possible combustion mechanism was proposed. This paper demonstrates the efficacy of Ti in improving material energy output, longer self-sustained combustion, reducing ignition delay and promoting catalytic activity of thermal decomposition. The exploration results are expected to propose a new development route in the field of solid propellants.

Experimental section

Materials

Among the materials used in the experiment, perchloric acid and Ti-MPs (300 mesh, purity 99.9%) were purchased from Shanghai Aladdin Biochemical Technology Co., Ltd. AP was purchased from Sinopharm Chemical Reagent Co., Ltd. All chemicals and powders are used immediately upon receipt.

Preparation of composite system samples containing Ti-MPs

Preparation of DAP-4/Ti powder

First, DAP-4 was synthesized by the method previously reported [27]. Before the experiment, the stoichiometry ratio of DAP-4 and Ti in the ideal state of complete reaction was calculated in Eq. (1) and the mass ratio of Ti to oxidant was obtained as 4: 6.

$$Ti + 2O \rightarrow TiO_2 \quad (1)$$

The mixed powder was prepared by a simple physical dry mixing method. According to the calculated formula, DAP-4 and Ti were added to the agate mortar for grinding, continuous grinding and stirring until the components were uniformly dispersed. The test mass was 0.4 g, and the calorimeter was tested in a closed natural environment (without oxygen). A total of nine groups of detonation heat values with different ratios were obtained (as shown in Fig. 1a). Apparently, when the mass ratio of Ti to oxidant is 0.45: 0.55, the mixed powder has the highest heat of combustion, releasing 985 J g^{-1} more heat than the 8128 J g^{-1} of pure DAP-4. This ratio is higher than the ideal stoichiometric ratio of 0.4: 0.6, indicating that other elements are involved in the reaction during the combustion process, releasing

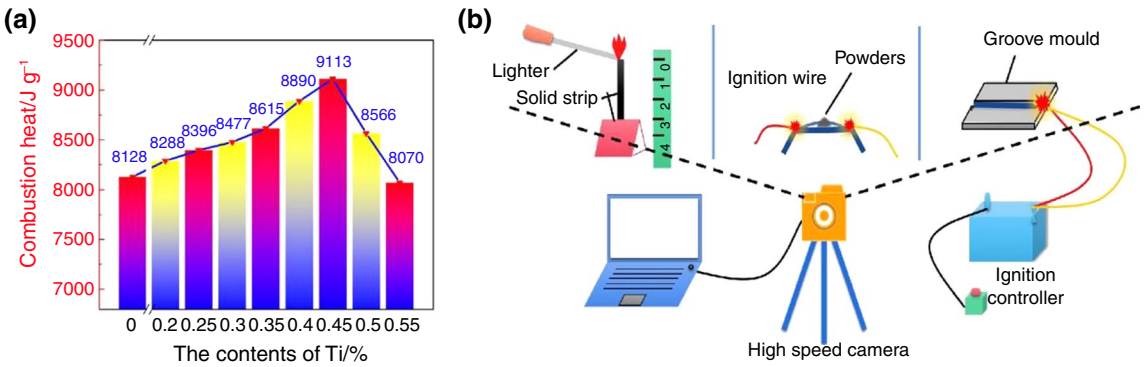

Fig. 1 Calorimetric value of oxygen bomb for different formulations (**a**). Combustion experiment schematic diagram (**b**)

more heat. With the increase of Ti content, the heat of combustion first increased and then decreased sharply. When DAP-4/Ti mass ratio is 0.55: 0.45, the heat release dropped to 8,070 J g^{-1}. This shows that the addition of Ti metal can improve the energy release of the propellant within a reasonable specific gravity range. The DAP-4/Ti mass ratio of 0.55: 0.45 was chosen for the follow-up experiments, and five other formulations were investigated. The selected formulations are shown in Table 1.

Preparation of F/DAP-4/Ti solid strip

Designed with constant binder content (10%). The F/DAP-4/Ti composites were prepared by changing the formulation by mixing DAP-4/Ti powder with fluoroelastomer solution [28]. First, crush an appropriate amount of fluorine rubber, pour it into ethyl acetate solvent, and leave it at room temperature for 12 h until the rubber particles are completely dissolved. Add the pre-mixed DAP-4/Ti powders, and shake it by ultrasonic cleaning machine sonic waves for 3 h to get a well-mixed slurry. The rheological properties of the slurry were adjusted by adding ethyl acetate. The slurry was pressed into a self-made aluminum alloy mold (2 mm × 2 mm × 47 mm), and the finished sample was maintained in a constant temperature oven at 60 °C. A dense composite polymer solid strip sample was obtained after demolding. The prepared solid strip formulations were shown in Table S1.

Characterization

The microstructure and morphology of DAP-4/Ti powder and F/DAP-4/Ti composites were characterized by scanning electron microscopy (SEM + EDX). The samples were sprayed with gold prior to being observed. Powder X-ray diffraction (XRD) spectra were collected on a Philips X Pert Pro X-ray diffractometer using Cu-Kα (40 kV, 40 mA) radiation.

The variation of physical properties of DAP-4/Ti hybrid powder and F/DAP-4/Ti composites with temperature was examined by TG-DSC technique. The experiment was realized on NETZSCH STA 449F3 STA449F 3A-0971-M. The test sample mass is 0.3–0.5 mg. The test temperature range is 40–500 ℃, and the heating rate is set at 10 ℃ min^{-1}.

Table 1 Mixed powder system formula

No	Mass/%	
	DAP-4	Ti
DAP-4	100	0
DAP-4/Ti-1	75	25
DAP-4/Ti-2	65	35
DAP-4/Ti-3	55	45
DAP-4/Ti-4	45	55

Flame morphology and propagation were captured with a high-speed camera (Revealer X113) with a sampling rate of 1000 frames sec^{-1} (powder) and 500 frames sec^{-1} (solid strip). Ignition was heated with a nichrome wire. The schematic diagram is shown in Fig. 1b. The burning rate of DAP-4/Ti powder and F/DAP-4/Ti composites were calculated based on the flame propagation distance and time. The sample was ignited with an electrode of 24 V DC voltage. In the combustion chamber, the electrode ignites about 50 mg of the sample and the variation of pressure is observed.

Characterization results

In this paper, we characterized the morphology and structure of DAP-4/Ti powder and F/DAP-4/Ti composite solid. The experiments started with the synthesis of the perovskite energetic material DAP-4 at room temperature, and the crystalline particles were regular cubes with sharp angles, smooth surfaces, and well-defined structures as seen in Fig. 2a. In Fig. 2b, it can be clearly observed that the Ti are refined into small pieces and have uneven particle size distribution, rough surface, cracks, and lamellar structure on the particle surface. Figure 2c shows the state of the two raw materials after physical mixing. A small amount of Ti particles adhered to the surface of DAP-4 without obvious aggregation. It can be seen that the powder is well mixed.

The crystal structures of pure DAP-4, Ti and DAP-4/Ti mixed powder were measured by XRD, as shown in Fig. 3. Among the main diffraction peaks of the composite system, the mountains were at 21.44°, 24.67°, 27.7°, 36.88°, and 39.40° reflected from (222), (400), (420), (531), and (600) of the $(H_2dabco)[NH_4(ClO_4)_3]$, these results are in general agreement with those of the XRD model (CCDC: 1,528,108) [29]. It was demonstrated that the crystal structure of the prepared DAP-4 belongs to the ABX_3 molecular perovskite structure. The protonated H_2dabco^{2+} is the A cation in the cell, NH_4^+ is the B cation, and ClO_4^- is the X bridge. Each NH_4^+ is surrounded by 12 O atoms in 6 ClO_4^-. ClO_4^- can be seen as a bridge between the two ambient NH_4^+, forming a three-dimensional cage-like supra-molecular framework. The protonated H_2dabco^{2+} is locked in the cubic cage-like space. The above results indicate that the perovskite molecule DAP-4 was successfully synthesized by a simple one-pot reaction. Analyzing the XRD measurements corresponding to the received Ti, the peaks were at 35.19°, 38.70°, 40.32°, 53.13°, 63.12°, 70.72°, 76.27° and 77.47° reflected from (100), (002), (101), (102), (110), (103), (112) and (201) planes of Ti, this result corresponds to the standard PDF card 44–1294. The absence of obvious oxide layers (TiO, TiN, TiO_2) on the surface contributes to the accuracy of the experimental results. The XRD results of the mixed powder showed that the lattice structures of DAP-4 and Ti remained unchanged during the preparation.

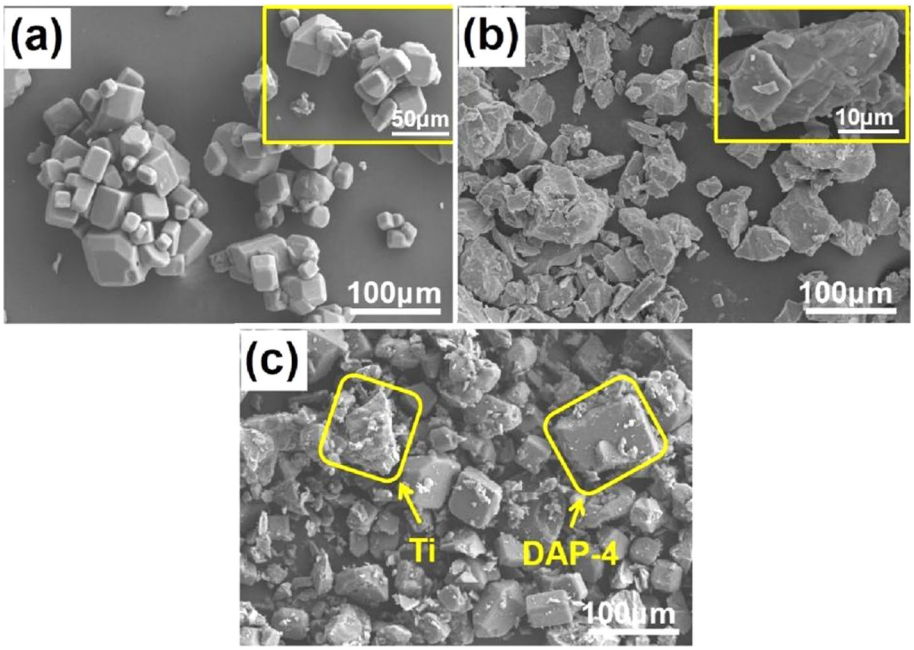

Fig. 2 SEM images of pure DAP-4 (**a**), Ti-MPs (**b**) and DAP-4/Ti (**c**)

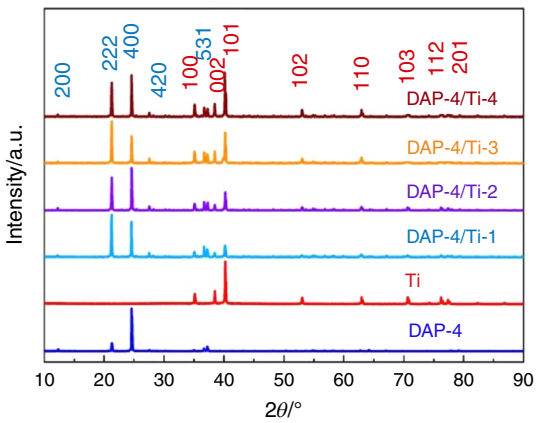

Fig. 3 XRD curves of powders

The composite material of F/DAP-4/Ti composites was constructed, and the cross-sectional area of these solid strips was relatively uniform. Fig. S1a is a solid strip of pure DAP-4 with a darker overall color, and Fig. S1b-e are SEM images of composites with the different mass ratios of DAP-4 and Ti. DAP-4 was mixed with Ti to make a uniform distribution. In the figure, we can see the rough surface with some larger diameter DAP-4 particles. This is because DAP-4 cannot be mechanically ground to smaller micron sizes. In addition, pores between the particles can be observed in the cross section of the composite due to the volatilization of the solvent. The porosity helps to improve the heat and mass transfer during the combustion process, thus increasing the combustion rate. The XRD peaks of the solid composite strips shown in Fig. S1f are consistent with those of the powder.

The elemental composition and dispersion of the F/DAP-4/Ti-4 composite cross-sections were determined using energy-dispersive X-ray spectrometer (EDX). The EDX shown in Fig. S2b-d indicates the presence of Ti, Cl and O as structural elements of the composite solid material and the expected peak of F due to F_{2602}. The distribution of Ti elements is relatively uniform, and the content distribution of F elements is small. The characteristic peaks of C, N, O, Cl, F and Ti elements are shown in Fig. S2e. The Ti content was small but the characteristic peaks were clearly discernible. qualitative EDX analysis showed that the Ti and O were 30.35% and 23.84% (mass percentage), respectively. The contents of other elements of C, N, Cl and F were 13.7%, 4.93%, 12.39% and 14.81%, respectively. It was demonstrated that the composite sample materials required for the experiments were successfully prepared by a simple and easy method.

Results and discussions

Combustion performance study

The combustion performance of the propellant component is a necessary process that affects the energy and pressure output of the entire material. The electrode combustion properties were investigated using a high-speed camera and the flame shape after electrode ignition was recorded. Since the electrode ignition is a transient action, the combustion of the material is defined as self-sustained combustion. The combustion process of the flame is divided into five stages:

ignition, development, stable combustion, weakening and extinction.

Figure 4 shows the electrode ignition combustion process of a 50 mg mound-like composite powder sample. From Fig. 4a, it can be noticed that the flame morphology of pure DAP-4 is relatively regular. The flame zone in the front view is in the shape of a small strip with the flame root close to the crucible contact surface. It takes only 85 ms to reach the fierce point where the flame burns steadily. The whole process is concise and clear, and the response is rapid and intense. The interior of the fireball is in a dazzling incandescent state, with a large incandescent area in the center, which is very bright during the development and stabilization phase.

Figure 4b–e show the ignition combustion process of the mixed powder after adding metal Ti under the same conditions. It can be seen that the combustion time of the sample becomes longer, the bright area becomes larger and the shape is irregular after the addition of metal powder. In general, the middle incandescent region is more dazzling. A large number of sputtering spark particles are observed in the developing and stable combustion phase, which is due to the fluctuation of the gas flow and the sputtering phenomenon of combustion particles by the combustion products of DAP-4, such as CO_2. The gas expansion causes the combustion particles to move upward, creating a trajectory of combustion particles moving into the surrounding space [30]. During the flame weakening phase, it can be observed that it is accompanied by the sputtering of unburned particles and the simultaneous generation of a large amount of smoke. The smoke is a combination of adhesion and condensation of moisture and particles in the DAP-4 combustion products and spreads in space with the influence of the airflow. In the comparison of DAP-4/Ti, the composite powder containing 45% Ti (DAP-4/Ti-3) showed a continuous burning time of up to 265 ms, which is 100 ms longer than that of pure DAP-4. This may be due to the relatively slow burning of the metal particles. The shortest continuous combustion of the composite powder (DAP-4/Ti-2) containing 35% Ti is 185 ms, which is 20 ms longer than that of pure DAP-4. When Ti reacts with oxygen, a protective TiO_2 film is formed on the surface. When the surface of the particles acts as a protector, the combustion and rate of the particles are limited. Only when the temperature exceeds the melting point of the oxide, the surface layer loses its protective effect.\

The 0.3 g of powder was laid flat in the template slot and ignited with an electrode at one end. The flame front propagation is shown in Fig. 5. As can be seen in Fig. 5a, the flame front of pure DAP-4 reached the other end with

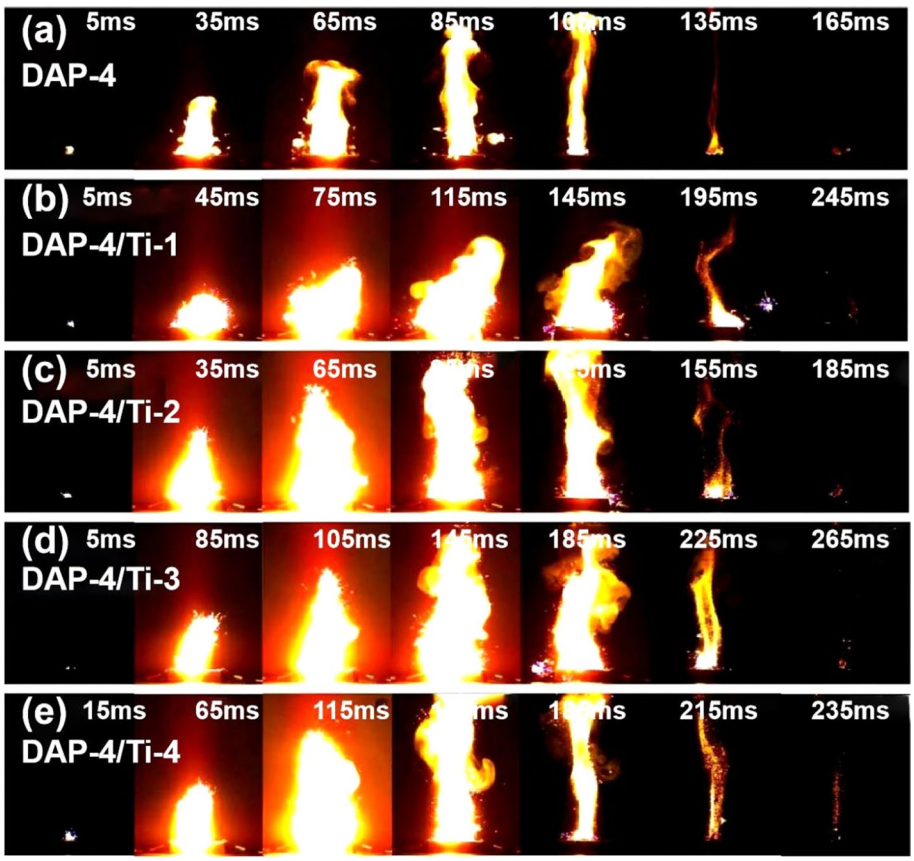

Fig. 4 High-speed photographic images of 50 mg powders electrode ignition (**a**–**e**)

a continuous burning at the ignition point and an overall regular triangular cross section. With the increase of Ti, the flame burning intensity increases and the burning space expands as shown in Fig. 5b–e. At the same time, the flame shape is irregular and the incandescent region is more dazzling. There are also many sputtering spark particles at the edge of the burning area. As the combustion wave spreads outward, tiny particles of slow-burning titanium metal powder are ejected from the combustion zone. The escaped particles become burning spheres and fall freely into the air.

According to the dynamic propagation of the flame front in Fig. 5, the flame propagation velocity calculated by taking the steady-state propagation phase of the flame is shown in Table S2. Due to the fast propagation of the internal combustion wave of titanium powder, the heat energy transfer and mass transfer between the particles is fast. The front end of the flame can quickly accumulate heat and reach the ignition point. Obviously the metal gives full play to its high heat and mass transfer in the flame propagation process, making the flame propagation speed of 0.169 mm ms^{-1} for the powder containing 55% Ti.

The flame dynamics of the composite ignited by an open flame are shown in Fig. 6a-e, and the burn rate is shown in Fig. 6f. It can be seen that there is a process of energy accumulation and slower flame propagation in the early phase of combustion of the composite. The flame intensity of the solid strip at 0.2 s is much higher than that of the pure DAP-4 at 0.4 s. As the flame front advances, the combustion reaction becomes very intense and the combustion rate increases rapidly. With the addition of 25% Ti (F/DAP-4/Ti-1), the superior heat transfer rate of the metal shortened the combustion time by 0.8 s compared to that of pure DAP-4. However, with the continuous combustion of titanium, the longer the combustion time of the composite with more metal added. In the flame comparison of F/DAP-4/Ti, the composite containing 55% Ti (F/DAP-4/Ti-4) had a long duration, reaching 1.7 times that of the pure DAP-4 composite.

The decomposition of fluoroelastomers in this part of the combustion produces other hydrocarbon fuels. The decomposition gases consisting of fuel and oxidizer components are mixed together to form a diffusion flame on the combustion surface [31].

For high-energy materials, it is important to record the pressure curves during combustion. Fig. S3 shows the pressure curve of DAP-4/Ti, and the detailed data calculated according to Fig. S3 are shown in Table 2.

It can be seen from Fig. S3 that the pressure in the preliminary stage rises rapidly due to the high-temperature gas eruption immediately after the specimen ignition. With the addition of Ti, the peak pressure of DAP-4/Ti showed a slow decreasing trend. The rise time was only 7 ms for pure DAP-4, and increased to 19 ms for the addition of 55% Ti (DAP-4/Ti-4), which was 2.7 times higher than that of pure DAP-4. Similarly, the addition of 55% Ti (DAP-4/Ti-4) reduced the maximum explosion pressure of the mixed powder from 915.79 kPa for pure DAP-4 to 291.96 kPa. This may be due to the lack of oxygen supply to the oxidizer DAP-4.

Thermal properties

The thermal decomposition behavior profoundly affects the quality and shelf life of energetic materials. Figure 7 shows the TG and DSC curves of the composite samples DAP-4/Ti and F/DAP-4/Ti at a temperature increase rate of 10 ℃ min^{-1}. Figure 7a shows that the tested powder samples have a weak heat absorption peak around 274 ℃. At this time, the samples are not melted or extruded by organic processes, so the appearance of the heat absorption peak is most likely caused by changes in crystal morphology, and the addition of Ti metal powder does not affect the phase change of the crystal. The exothermic elevation temperature of pure DAP-4 was 380.8 ℃. The elevated exothermic temperature of the samples continued to decrease with increasing Ti content, but the effect was not particularly pronounced. The addition of 55% Ti (DAP-4/Ti-4) reduced the peak exothermic temperature by 6.2 ℃, indicating that the addition of Ti reduced the peak exothermic temperature to some extent. Figure 7b shows the TG curves of the composite powder samples, in which the initial decomposition of the powder containing 25% Ti (DAP-4/Ti-1) is close to 50 ℃. With the increase of Ti, the initial decomposition temperature of the composite samples gradually increases, and the initial temperature of

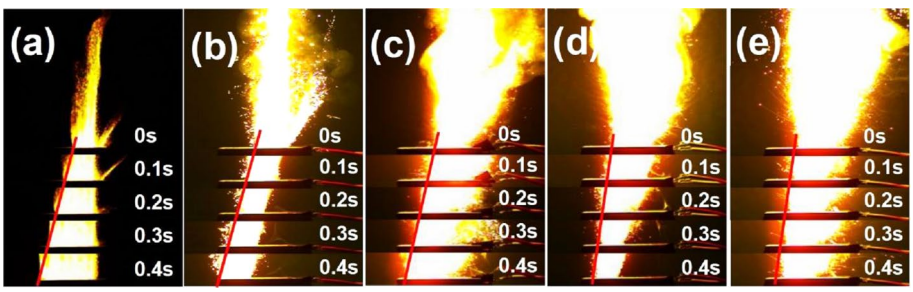

Fig. 5 High-speed photographic imges of 0.3 g powders electrode ignition: DAP-4 (**a**) and DAP-4/Ti (**b**–**e**)

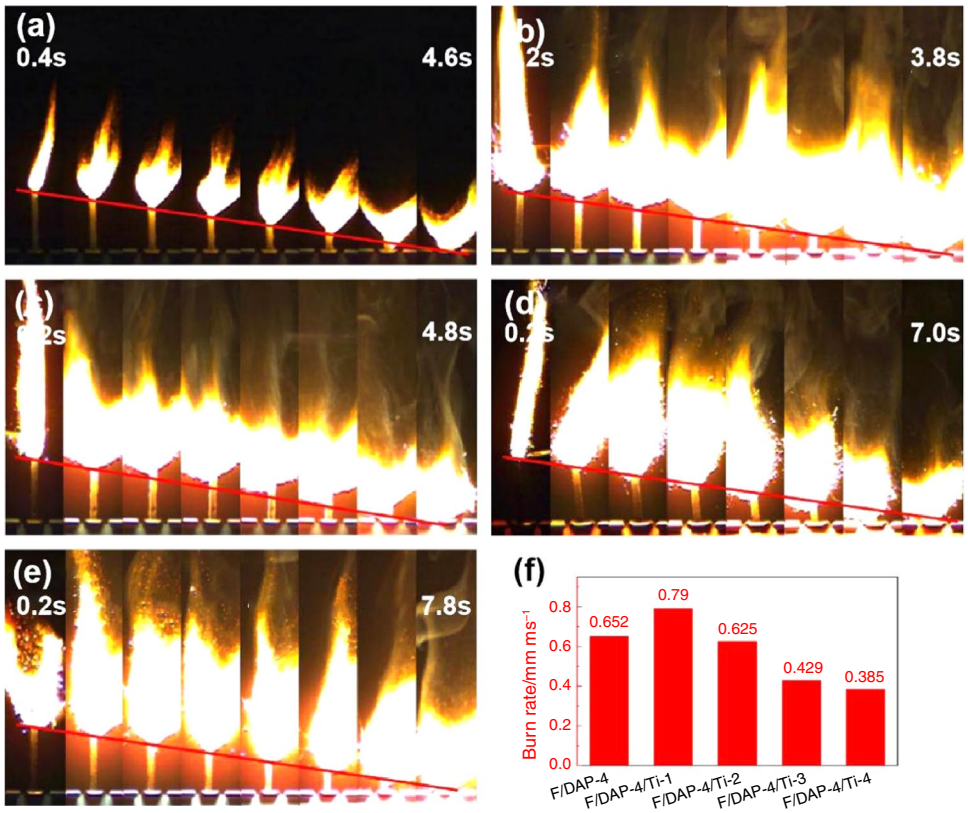

Fig. 6 High-speed photographic images of 3 cm polymer flame ignited by open flame (**a**–**e**) and burn rate (**f**)

Table 2 The curve data for the rise time, P_{max}, and pressurization rate from **Fig. S3**

Sample	Rise time/ms	P_{max}/kPa	Pressurization rate/kPa ms^{-1}
DAP-4	7	915.79	130.21
DAP-4/Ti-1	8	526.89	65.40
DAP-4/Ti-2	14	435.50	30.01
DAP-4/Ti-3	14	409.12	28.96
DAP-4/Ti-4	19	291.96	15.04

thermal decomposition of the powder containing 55% Ti is close to 325.4 ℃ of pure DAP, but its thermal decomposition termination temperature is similar to that of pure DAP-4, which are both around 385 ℃.

The mass loss rate of the composite powder was 70%, 58.5%, 51.9% and 38.1% for Ti content of 25, 35, 45 and 55%, respectively, while the mass loss rate of pure DAP-4 was 81.4%. In the combustion reaction of DAP-4 with Ti, elements such as O, N and Cl were involved in the chemical reaction. These elements react with titanium to form solid products, such as TiO_2, reducing the production and release of gases.

Figure 7c shows the DSC curves of the solid strips, where the phase change heat absorption peaks are still present at around 274 ℃. The peak exothermic temperatures of the composites were 372.5 371.4 364.6 and 360.4 ℃, respectively, and the peak exothermic temperature of the solid strip of F/DAP-4 was 381.5 ℃. The peak temperature of the composite with 49.5% Ti (F/DAP-4/Ti-3) was significantly lower by 21.1 ℃. This indicates that the catalytic effect of thermal decomposition gradually increases with the increase of Ti content in the samples. We can also find that the addition of F_{2602} reduces the decomposition peak from 374.6 to 360.4 ℃, indicating that the addition of binder also has a specific effect on the thermal decomposition of DAP-4/Ti. In Fig. 7d, the initial temperatures of thermal decomposition of the composites with Ti content of 22.5, 31.5, 40.5 and 49.5% were 38.6, 323.1, 321 and 322.0 ℃, respectively. The termination temperatures of thermal decomposition were 385.8, 383.2, 381.4 and 376.0 ℃, respectively. The decomposition temperature differences were 152.2, 80.4, 77.5 and 73.2 ℃, respectively. Therefore, it can be found that

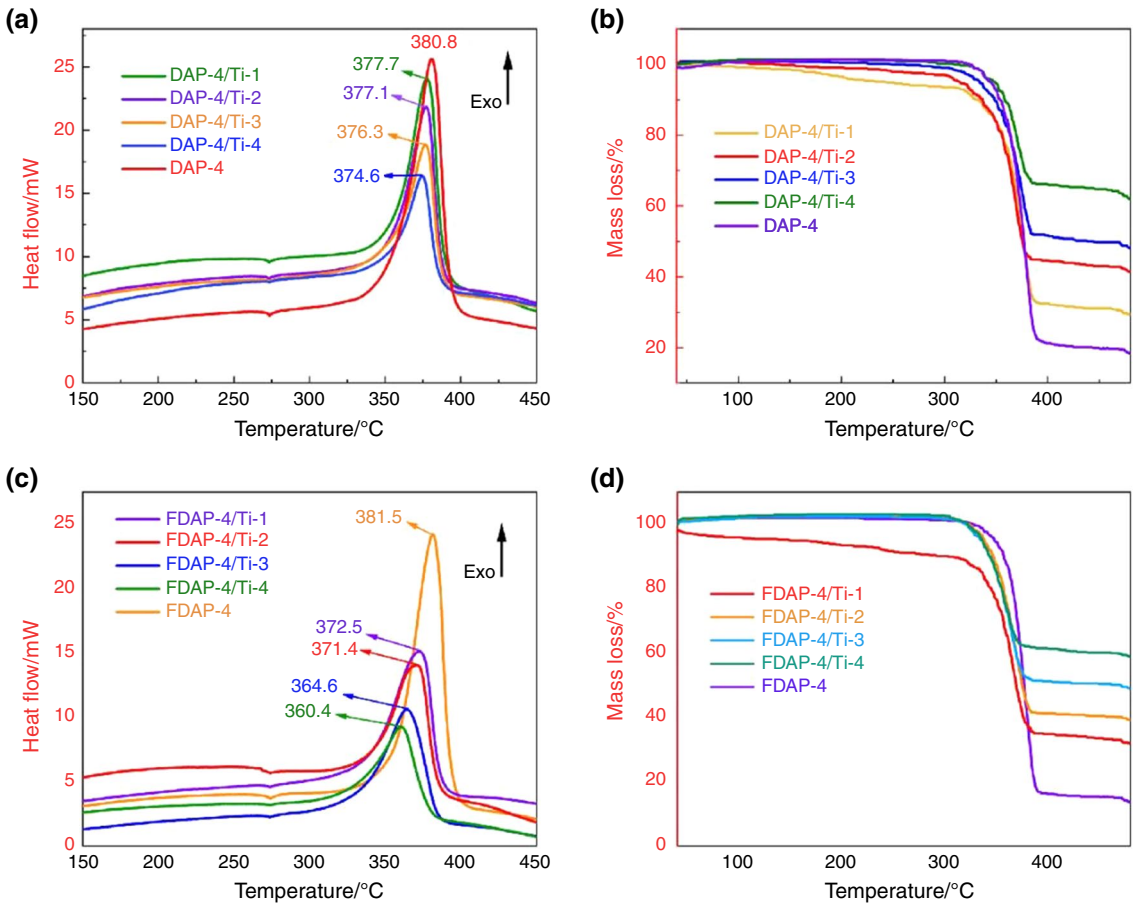

Fig. 7 TG-DSC curves of DAP-4/Ti (**a**, **b**) and F/DAP-4/Ti (**c**, **d**)

the combustion rate of F/DAP-4/Ti was effectively increased with the increase of Ti content.

Combustion condensation products analysis

In order to more fully understand the chemical reactions between DAP-4 and Ti, we collected the combustion products and dried them in an oven for 24 h. The solid condensation products were tested by SEM, EDS and XPS. The gaseous products of the thermal decomposition process were examined by MS and the following results were obtained:

It can be observed in Fig. 8 that there is a bonding phenomenon between DAP-4 particles after a short period of high temperature combustion, and there is a partially reacted incomplete cubic structure. The metal particles grow spherically, forming spherical, large particles of oxide [32].

The EDS elemental analysis of Fig. 9 revealed the highest coverage of Ti and O elements on the surface of the spheres, which further proves that the generated spheres are TiO_2 oxides.

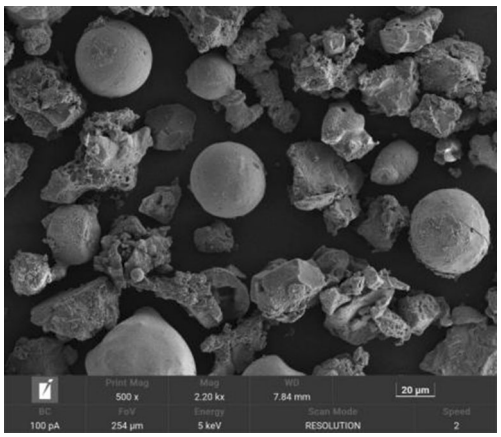

Fig. 8 SEM images of DAP-4/Ti combustion products

The combination of XPS features was utilized to be able to identify the condensation product material composition, as shown in Fig. 10. The two main peaks at 284.8 and 531.2 eV were identified as the C1s and O1s peaks, with the greatest peak intensity for elemental oxygen, indicating

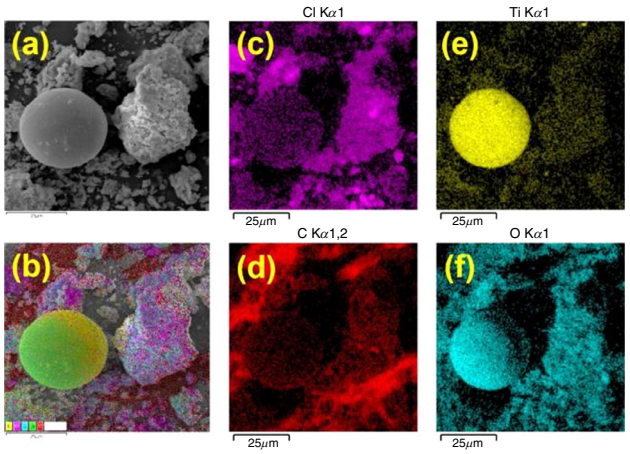

Fig. 9 EDS images of DAP-4/Ti combustion products

the highest O content, which is consistent with the EDS results. The binding energies were similar at 200 eV and 458.5 eV, and two main peaks were identified as Cl2p and Ti2p, respectively. The orbital binding energies of Ti2p are 464.3 and 458.6 eV, respectively, which suggests that Ti exists mostly in the tetravalent form in the product.

In order to gain a more complete understanding of the thermal decomposition and reaction mechanism of the samples, we measured the gas MS curves of the decomposition products, as shown in Fig. 11. The curves in the figure can be observed that during the thermal decomposition reaction of DAP-4 and Ti, gases such as N_2, H_2O, CO_2, HCl, NO_2, NO, HClO are mainly generated, and these gas products are released by the decomposition of DAP-4 [33–35]. The unique cage-like structure of molecular chalcocite reacts with metal fuel combinations to produce stable oxides can and a variety of gaseous products, releasing higher energy [36, 37].

Study on combustion decomposition mechanism

In general, the surface area of the metals decreases rapidly due to their sintering properties. However, since the Ti metal itself burns without severe sintering, it still has a high concentration of dislocations and a large surface area after mixing with DAP-4. This may lead to enhanced oxygen diffusion and increased transient energy release potential. A possible combustion decomposition mechanism was proposed by studying the characterization data of DAP-4/Ti and F/DAP-4/Ti composites. The preliminary exploration of the combustion decomposition mechanism is shown in Fig. 12.

During the warming process, the activated proton H_2dabco^{2+} breaks the cage state when the heating energy is sufficient to break the cage state formed by the Coulomb interaction between $ClO_4^-$and NH_4^+ in the anion skeleton. As the ambient temperature increases, the presence of Ti and the resulting oxide layer accelerates the transfer of protons, resulting in the formation of more perchloric acid, which is more likely to produce superoxide radicals. And the superior heat transfer characteristics of Ti metal make it transfer heat faster, while the liquid product decomposes and sublimates into gaseous $HClO_4$ and NH_3. Simultaneous solid–gas multiphase reactions occur, producing large amounts of N_2O, Cl_2, O_2, HCl, H_2O, and small amounts of NO. The gas-phase reactions produce large amounts of NO, Cl_2, O_2, H_2O, etc. In most cases, O_2 and Cl_2 can be preferentially absorbed by metallic materials due to their higher activity compared to products such as CO and H_2O. The superior affinity of titanium for oxygen allows the reaction to produce more TiO_2, which leads to faster and higher exothermic reactions and less mass loss. Ti maintains its structure under rapid heating at high temperatures, which may lead to a lower ignition temperature and enhanced ignition capacity of titanium during combustion.

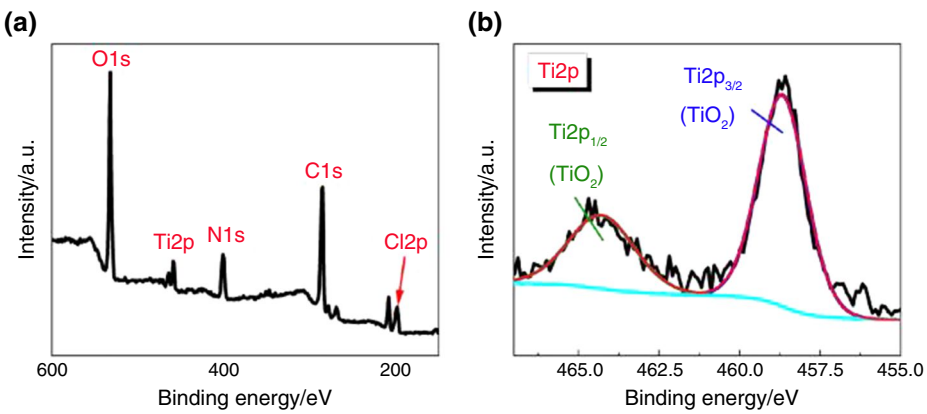

Fig. 10 XPS full spectrum (**a**) and the high-resolution Ti2p (**b**)

It can be seen that Ti catalyzes the reaction between the gas-phase decomposition products rather than the solid-phase melt of DAP-4 itself, and ignition is dependent on gas-phase interactions. The energy released by combustion increases significantly.

In conclusion, the presence of Ti increases the active sites on the oxidized surface. After ignition and heating, DAP-4 decomposes to release oxygen, which reacts with the metal oxide layer and Ti. During this period, once the temperature and energy are able to break the oxide layer, the protective layer of the metal becomes useless, allowing the Ti core to join the reaction and release more energy. It can be seen that the chemical reaction of the Ti metal particles gradually moves from the surface oxide layer to the core. The results show that the molecular perovskite energetic material DAP-4-based Ti powder composites have good combustion performance and more considerable energy output. From the application point of view, Ti has a high characteristic specific enthalpy of combustion and can be a choice to replace or supplement materials such as Al and Mg. Of course, it can also be used to develop new materials with improved performance, safety and stability.

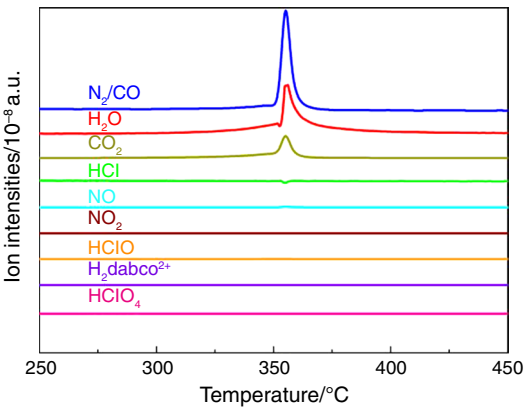

Fig. 11 The MS curve of DAP-4/Ti with a temperature rate of 10 ℃ min^{-1}

Conclusions

In summary, the combustion performance of DAP-4-based titanium powder composites was investigated, and a possible combustion mechanism was proposed. The homogeneously mixed DAP-4/Ti hybrid powder was successfully prepared, and the F/DAP-4/Ti stable solid composites were successfully prepared with the polymer binder F_{2602}. Characterization and experimental tests showed that the addition of metal Ti to DAP-4 could effectively enhance the combustion heat and flame luminescence intensity of the composites. The presence of Ti particles can regulate the combustion rate of DAP-4 and accelerate the dynamic flame propagation, while extending the self-sustained combustion time of the composites. The presence of Ti regulates the burning rate of DAP-4, accelerates the dynamic flame propagation and prolongs the self-sustained burning time of the composite. At the mass ratio of Ti to DAP-4 of 0.45:0.55, the heat of combustion of DAP-4/Ti-3 was the highest at 9,113 J g^{-1}. The combustion duration of 50 mg of pure DAP-4 was 165 ms, while the self-propagating combustion duration of DAP-4/Ti-3 could reach 265 ms with the addition of 45% Ti. The analysis of the combustion rate of the mixed powder showed that that the front propagation speed of DAP-4/Ti-3 flame could reach 0.225 mm ms^{-1}. However, the combustion rate of DAP-4/Ti gradually decreased with the increase of Ti. When the Ti particle addition was 55%, the boosting rate decreased significantly to 15.04 kPa ms^{-1}. In addition, when the mass ratio of F_{2602}/Ti/DAP-4 was 10: 49.5: 40.5, the combustion rate of the composite was the slowest at 0.385 mm ms^{-1}. TG-DSC showed that with the addition of Ti, the combustion rates of DAP-4/Ti and F/DAP-4/Ti composites decomposition temperature gradually decreased with the addition of Ti. Studies have shown that DAP-4-based Ti composites have good combustion performance and energy release and that metallic titanium particles are a viable alternative fuel for high energy solid propellants.

Supplementary Information The online version contains supplementary material available at https://doi.org/10.1007/s10973-023-12572-9.

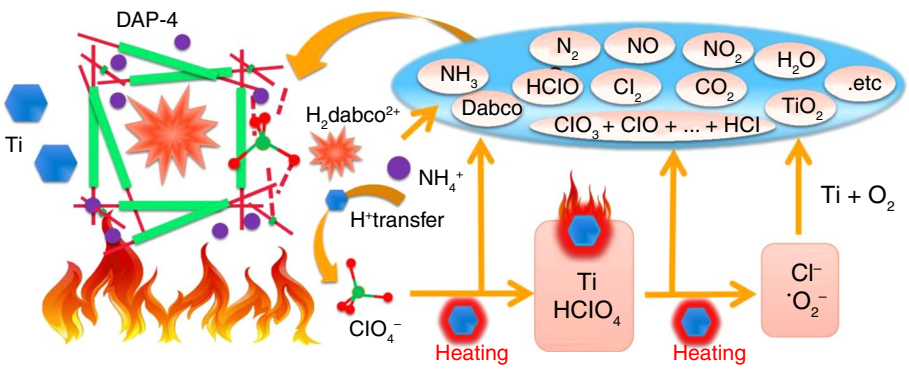

Fig. 12 Combustion mechanism diagram of DAP-4/Ti

Acknowledgements This work was supported by the National Natural Science Foundation of China (No. 52276138) and the Fundamental Research Program of Shanxi Province (No. 20210302123030, 202203021212160). Authors thank Dr. Peng Deng of Beijing Institute of Technology for his help in experiment.

Data availability statement The raw/processed data required to reproduce these findings cannot be shared at this time as the data also forms part of an ongoing study.

Declarations

Conflict of interest The authors declare no conflict of interest.

Ethical approval Ethics approval was not required for this research.

References

1. Yadav N, Srivastava PK, Varma M. Recent advances in catalytic combustion of AP-based composite solid propellants. Defence Technol. 2021;17(3):1013–31. https://doi.org/10.1016/j.dt.2020.06.007.
2. Jos J, Mathew S. Ammonium nitrate as an eco–friendly oxidizer for composite solid propellants: promises and challenges. Crit Rev Solid State Mater Sci. 2017;42(6):470–98. https://doi.org/10.1080/10408436.2016.1244642.
3. Chaturvedi S, Dave PN. Solid propellants: AP/HTPB composite propellants. Arab J Chem. 2019;12(8):2061–8. https://doi.org/10.1016/j.arabjc.2014.12.033.
4. Vara JA, Dave PN, Ram VR. Nanomaterials as modifier for composite solid propellants. Nano Struct Nano Objects. 2019;20: 100372. https://doi.org/10.1016/j.nanoso.2019.100372.
5. He Q, Wang J, Mao Y, et al. Fabrication of gradient structured HMX/Al and its combustion performance. Combust Flame. 2021;226:222–8. https://doi.org/10.1016/j.combustflame.2020.12.003.
6. Severac F, Alphonse P, Estève A, et al. High-energy Al/CuO nanocomposites obtained by DNA-directed assembly. Adv Func Mater. 2012;22(2):323–9. https://doi.org/10.1002/adfm.201100763.
7. Dong H, Xia M, Wang C, et al. Al/NiO nanocomposites for enhanced energetic properties: Preparation by polymer assembly method. Mater Des. 2019;183: 108111. https://doi.org/10.1016/j.matdes.2019.108111.
8. Pang W, De Luca LT, Fan X, et al. Effects of different nano-sized metal oxide catalysts on the properties of composite solid propellants. Combust Sci Technol. 2016;188(3):315–28. https://doi.org/10.1080/00102202.2015.1083986.
9. Mahdavi M, Farrokhpour H, Tahriri M. Investigation of simultaneous formation of nano-sized CuO and ZnO on the thermal decomposition of ammonium perchlorate for composite solid propellants. J Therm Anal Calorim. 2018;132(2):879–93. https://doi.org/10.1007/s10973-018-7018-0.
10. Valluri SK, Ravi KK, Schoenitz M, et al. Effect of boron content in B· BiF_3 and B· Bi composites on their ignition and combustion. Combust Flame. 2020;215:78–85. https://doi.org/10.1016/j.combustflame.2020.01.026.
11. Swetha BN, Keshavamurthy K, Gupta G, et al. Silver nanoparticles enhanced photoluminescence and the spectroscopic performances of Nd_3^+ ions in sodium lanthanum borate glass host: Effect of heat treatment. Ceram Int. 2021;47(15):21212–20. https://doi.org/10.1016/j.ceramint.2021.04.124.
12. Zhou X, Torabi M, Lu J, et al. Nanostructured energetic composites: synthesis, ignition/combustion modeling, and applications. ACS Appl Mater Interfaces. 2014;6(5):3058–74. https://doi.org/10.1021/am4058138.
13. Yuan X, Meng L, Zheng C, et al. Deep insight into the mechanism of catalytic combustion of CO and CH_4 over $SrTi_{1-x}B_xO_3$ (B= Co, Fe, Mn, Ni, and Cu) perovskite via flame spray pyrolysis. ACS Appl Mater Interfaces. 2021;13(44):52571–87. https://doi.org/10.1021/acsami.1c14055.
14. Chen SL, Yang ZR, Wang BJ, et al. Molecular perovskite high-energetic materials. Sci China Mater. 2018;61(8):1123–8. https://doi.org/10.1007/s40843-017-9219-9.
15. Peng D, Guo X, Fang H, et al. Novel Role of Molecular Perovskite Energetic Materials: A Potential High-Energy Oxidant for the Solid Rocket Propellant. Available at SSRN 4000440.
16. Zhou J, Ding L, Zhao F, et al. Thermal studies of novel molecular perovskite energetic material $(C_6H_{14}N_2)[NH_4(ClO_4)_3]$. Chin Chem Lett. 2020;31(2):554–8. https://doi.org/10.1016/j.cclet.2019.05.008.
17. Li X, Hu S, Cao X, et al. Ammonium perchlorate-based molecular perovskite energetic materials: preparation, characterization, and thermal catalysis performance with MoS_2. J Energ Mater. 2020;38(2):162–9. https://doi.org/10.1080/07370652.2019.1679281.
18. Han K, Zhang X, Deng P, et al. Study of the thermal catalysis decomposition of ammonium perchlorate-based molecular perovskite with titanium carbide MXene. Vacuum. 2020;180: 109572. https://doi.org/10.1016/j.vacuum.2020.109572.
19. Zhu S, Cao X, Cao X, et al. Metal-doped (Fe, Nd, Ce, Zr, U) graphitic carbon nitride catalysts enhance thermal decomposition of ammonium perchlorate-based molecular perovskite. Mater Des. 2021;199: 109426. https://doi.org/10.1016/j.matdes.2020.109426.
20. Fang H, Guo X, Wang W, et al. The thermal catalytic effects of CoFe-Layered double hydroxide derivative on the molecular perovskite energetic material (DAP-4). Vacuum. 2021;193: 110503. https://doi.org/10.1016/j.vacuum.2021.110503.
21. Rehwoldt MC, Yang Y, Wang H, et al. Ignition of nanoscale titanium/potassium perchlorate pyrotechnic powder: reaction mechanism study. The Journal of Physical Chemistry C. 2018;122(20):10792–800. https://doi.org/10.1021/acs.jpcc.8b03164.
22. Yetter RA, Risha GA, Son SF. Metal particle combustion and nanotechnology. Proc Combust Inst. 2009;32(2):1819–38. https://doi.org/10.1016/j.proci.2008.08.013.
23. Girt E, Altounian Z, Swainson I P. The influence of the enthalpy of mixing on the Fe-substitution in $Nd_2Fe_{16.5}X_{0.5}$ (X= Al, Ti, Nb, W). Physica B: Condensed Matter. 1997; 234: 637–639. https://doi.org/10.1016/S0921-4526(96)01068-X.
24. Pantović Pavlović M R, Stanojević B P, Pavlovic M M, et al. Anodizing/Anaphoretic Electrodeposition of Nano-Calcium Phosphate/Chitosan Lactate Multifunctional Coatings on Titanium with Advanced Corrosion Resistance, Bioactivity, and Antibacterial Properties. ACS Biomaterials Science & Engineering. 2021; 7(7): 3088–3102. https://doi.org/10.1021/acsbiomaterials.1c00035.
25. Shafirovich E, Teoh SK, Varma A. Combustion of levitated titanium particles in air. Combust Flame. 2008;152(1–2):262–71. https://doi.org/10.1016/j.combustflame.2007.05.008.
26. Jacob R J, Zong Y, Yang Y, et al. Measurement of size resolved burning of metal nanoparticles for evaluation of combustion mechanisms//Proceedings of the 54th AIAA Aerospace Sciences Meeting, San Diego, CA, USA. 2016; 4–8. https://doi.org/10.2514/6.2016-0687.
27. Deng P, Wang H, Yang X, et al. Thermal decomposition and combustion performance of high-energy ammonium perchlorate-based

molecular perovskite. J Alloy Compd. 2020;827: 154257. https://doi.org/10.1016/j.jallcom.2020.154257.
28. Mao Y, He Q, Wang J, et al. Rational design of gradient structured fluorocarbon/Al composites towards tunable combustion performance. Combust Flame. 2021;230: 111436. https://doi.org/10.1016/j.combustflame.2021.111436.
29. Liu Y, Hu L, Gong S, et al. Study of Ammonium Perchlorate-based Molecular Perovskite (H_2DABCO)[$NH_4(ClO_4)_3$]/Graphene Energetic Composite with Insensitive Performance. Central European Journal of Energetic Materials. 2020; 17(3). https://doi.org/10.22211/cejem/127934.
30. Gao D, Wei X, Liu J, et al. Laser ignition and combustion characteristics of B-Al compound powder without and with HMX: a comparative study. Aerosp Sci Technol. 2022;120: 107268. https://doi.org/10.1016/j.ast.2021.107268.
31. Chaturvedi S, Dave PN, Patel NN. Thermal decomposition of AP/HTPB propellants in presence of Zn nanoalloys. Appl Nanosci. 2015;5(1):93–8. https://doi.org/10.1007/s13204-014-0296-3.
32. Duan H, Lin X, Liu G, et al. Synthesis of Ni nanoparticles and their catalytic effect on the decomposition of ammonium perchlorate. J Mater Process Technol. 2008;208(1–3):494–8. https://doi.org/10.1016/j.jmatprotec.2008.01.011.
33. Reid DL, Kreitz KR, Stephens MA, et al. Development of highly active titania-based nanoparticles for energetic materials. J Phys Chem C. 2011;115(21):10412–8. https://doi.org/10.1021/jp200993s.
34. Chen S, An T, Gao Y, et al. Gaseous products evolution analyses for catalytic decomposition of AP by graphene-based additives. Nanomaterials. 2019;9(5):801. https://doi.org/10.3390/nano9050801.
35. Zhang WJ, Li P, Xu HB, et al. Thermal decomposition of ammonium perchlorate in the presence of $Al(OH)_3$· $Cr(OH)_3$ nanoparticles. J Hazard Mater. 2014;268:273–80. https://doi.org/10.1016/j.jhazmat.2014.01.016.
36. Zhai P, Shi C, Zhao S, et al. Thermal decomposition of ammonium perchlorate-based molecular perovskite from TG-DSC-FTIR-MS and ab initio molecular dynamics. RSC Adv. 2021;11(27):16388–95. https://doi.org/10.1039/D0RA10559G.
37. Dennis C, Bojko B. On the combustion of heterogeneous AP/HTPB composite propellants: a review. Fuel. 2019;254: 115646.